



## OPEN ACCESS

## EDITED BY

Chaolong Zhang,  
Anqing Normal University, China

## REVIEWED BY

Xun Wu,  
Central South University, China  
Meng Zhang,  
Xi'an Jiaotong University, China  
Zhao Dongdong,  
Northwestern Polytechnic University,  
United States

## \*CORRESPONDENCE

Youmin Zhang,  
ymzhang@encs.concordia.ca

## SPECIALTY SECTION

This article was submitted to Smart Grids,  
a section of the journal Frontiers in Energy  
Research

RECEIVED 15 July 2022

ACCEPTED 02 August 2022

PUBLISHED 07 September 2022

## CITATION

Chen C, Song Y, Zhang Y, Tian J, Gao S and  
Lang B (2022), Adaptive fault-tolerant  
control of five-phase permanent magnet  
synchronous motor current using  
chaotic-particle swarm optimization.  
*Front. Energy Res.* 10:994629.  
doi: 10.3389/fenrg.2022.994629

## COPYRIGHT

© 2022 Chen, Song, Zhang, Tian, Gao and  
Lang. This is an open-access article  
distributed under the terms of the [Creative  
Commons Attribution License \(CC BY\)](#). The  
use, distribution or reproduction in other  
forums is permitted, provided the original  
author(s) and the copyright owner(s) are  
credited and that the original publication in  
this journal is cited, in accordance with  
accepted academic practice. No use,  
distribution or reproduction is permitted  
which does not comply with these terms.

# Adaptive fault-tolerant control of five-phase permanent magnet synchronous motor current using chaotic-particle swarm optimization

Chaobo Chen<sup>1,2</sup>, Ye Song<sup>2</sup>, Youmin Zhang<sup>1,3\*</sup>, Jiaqiang Tian<sup>4</sup>,  
Song Gao<sup>2</sup> and Baohua Lang<sup>2</sup>

<sup>1</sup>School of Automation and Information Engineering, Xi'an University of Technology, Xi'an, China,

<sup>2</sup>School of Electronic Information Engineering, Xi'an Technological University, Xi'an, China,

<sup>3</sup>Department of Mechanical, Industrial and Aerospace Engineering, Concordia University, Montreal, QC, Canada, <sup>4</sup>School of Electrical Engineering, Xi'an University of Technology, Xi'an, China

Both torque ripple and current harmonics are enlarged due to single-phase open-circuit fault of five-phase permanent magnet synchronous motor (FPMSM). Based on chaotic-particle swarm, an adaptive optimization fault tolerant control algorithm is proposed for the FPMSM current. First, Park and Clarke matrices are modified in coordinate transformation process. A reduced-order decoupling matrix is obtained under the open-circuit fault of FPMSM stator winding. Second, the fault-tolerant current is generated with the principle of constant magnetomotive force. Third, the current is adaptively optimized using chaotic-particle swarm algorithm. Hence, motor torque and motor current keep uniform steady state and dynamic performance with them in regular operation. Finally, numerical simulations are carried out to verify the effectiveness of the developed method.

## KEYWORDS

five-phase permanent magnet synchronous motors, chaos-particle swarm optimization algorithm, open-circuit fault, fault-tolerant control strategy, minimal torque ripple

## Introduction

The five-phase permanent magnet synchronous motor has the advantages of low torque ripple, multiple control degrees of freedom, and high efficiency (Liu et al. (2022); Zhang et al. (2021); Zhao et al. (2022)). It can achieve fault-tolerant operation without additional hardware support. Hence, it is widely used in industrial applications requiring high efficiency and reliability, such as systems in aerospace, energy conversion (Okedu Kenneth and Barghash, 2021), electric vehicle drive, etc. (Tao et al. (2019)). Among main body faults of a motor, the winding fault happens mostly. The faults include the winding open-circuit fault and the interturn short circuit fault. In particular, the winding open-circuit fault is the most common (Salehifar et al. (2014)).

The open-circuit fault of the motor winding will generate a large torque ripple. The heat generated by a large current usually causes irreversible demagnetization of permanent magnet (Huang et al. (2021)). These phenomena lead to a fast drop of control performance. Besides, the function of whole system is seriously affected. Therefore, it is necessary and critical to adopt an appropriate fault-tolerant control (FTC) strategy under fault conditions.

Field-oriented control (FOC) and direct torque control (DTC) are widely used in motor control strategies. At present, many advanced control strategies have been employed for fault-tolerant control of motors, including fuzzy control, adaptive control, model predictive control, etc. The principle of constant instantaneous torque was employed in (Zhao et al. (2011)). Lagrangian multiplication was used to obtain the expression of the fault-tolerant reference current. The ripple component was eliminated in output torque. However, the process is complicated. In addition, the method cannot work in the online case. A new coordinate transformation was developed in (Zhou et al. (2019)). The d-q axis current keeps unchanged before and after the phase failure. The torque remains intact at the moment of phase failure. However, it cannot guarantee the effect of suppressing the subsequent torque ripple. In (Gaeta et al. (2013)), three new coordinate transformations were proposed. A mathematical model was deduced for embedded PMSM after phase failure. Nevertheless, the influence of the third harmonic current is ignored. The effectiveness of the algorithm should be improved. Reference (Wu et al. (2019)) introduced a method of virtual voltage vector based on DTC. By optimizing its duty cycle and distributing the vector action time, it effectively suppressed the low-order harmonic current. Besides, it improved the utilization rate of the DC bus voltage, and widened the speed regulation range of the motor. Reference (Liu (2020)) designed a new direct torque control strategy based on matrix converter and DTC theory of PMSM. The developed method effectively suppressed torque fluctuations and made the system more robust. However, the above methods (Wu et al. (2019); Liu (2020)) lead to large ripple, due to the interaction of the fundamental current and the third harmonic back EMF in the FT-DTC method. Reference (Chen et al. (2021)) proposed a fault-tolerant control method combining quasi-proportional resonance and sliding mode observer. The method is suitable for the non-fault state of a motor. It can also accurately estimate the rotor position and motor speed in the event of a motor fault. In (Chen et al. (2019)), a model predictive torque control strategy was proposed, based on the voltage vector pre-screening. This method determined the sector position of the stator flux linkage and combined the transformation of torque and flux linkage amplitude. The corresponding voltage vector set was selected as the candidate vector of a prediction model by the look-up table method. The method effectively reduced the traversal times based on satisfying the control performance. However,

the selection of the weight coefficient reduced the adaptability of the algorithm. In (Fnaiech et al. (2010)), the fuzzy reasoning and sliding mode control theory was employed for the fault-tolerant control of winding phase-missing faults of six-phase induction motors. The system had robust stability. Besides, the tracking accuracy was improved. Unfortunately, the selection of fuzzy control parameters relied on expert experience and was highly subjective. Meanwhile, there was also the defect of high-frequency switching of sliding mode. Based on this, this paper proposes an adaptive fault-tolerant control of five-phase permanent magnet synchronous motor current using chaotic-particle swarm optimization.

The rest of the paper is arranged as follows: *FOC and coordinate transformation* Section corrects the Park and Clarke transformation matrices of FPMSM in the process of coordinate transformation. *Optimizing the reference current with the adjustment factor* Section solves the problem of phase loss of the motor in the FOC control framework, and at the same time, adaptively optimizes the solved fault-tolerant current using the adjustment factor. *Simulation and verification* Section builds a simulation in MATLAB/Simulink, and verifies the algorithm's feasibility through the simulation results and data. The conclusion of the thesis is given in *Conclusion* Section.

## FOC and coordinate transformation

Both the air gap magnetic field and the stator magnetic field have a coupling phenomenon in the flux linkage relationship, which leads to the vector control structure more complicated. **Figure 1** shows the schematic diagram of the system based on field-oriented control, where the motor is working normally, FOC is also known as vector control. The rotor field orientation is modeled on the control method of a DC motor. It uses coordinate transformation to decompose the stator current of an AC motor into a magnetic field component current and a torque component current, which are separately controlled. The magnetic flux current component and the torque current component are completely decoupled, to obtain the dynamic performance similar to the DC speed control system. The permanent magnet synchronous motor, established by coordinate transformation, can analyze the steady-state operation of the motor when the sine wave is input. The motor's instantaneous performance can also be analyzed.

## Mathematical model of five-phase permanent magnet synchronous motor

The basic idea of coordinate transformation is to convert relevant variables into the five-phase static coordinate system to the d-q rotating coordinate system for mathematical operations.

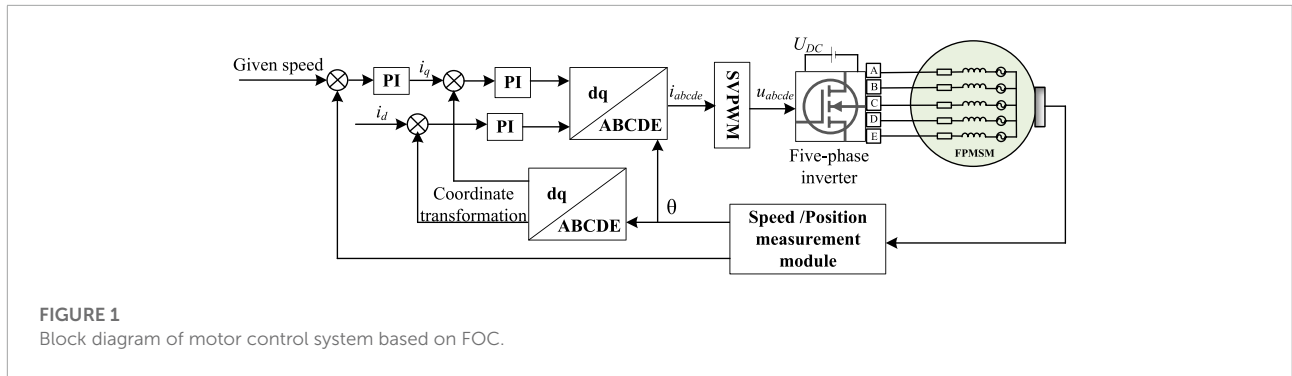


**FIGURE 1**  
Block diagram of motor control system based on FOC.

The d-q axis is a rotating coordinate system with synchronous rotational speed established by the synchronous rotation of the stator and rotor magnetic fields of the motor during coordinate transformation. The controller changes the voltage of the d-q axis to control the current of the d-q axis. However, in the end, the five-phase voltage of the motor can only be the voltage in the static coordinate system. Therefore, the corresponding inverse transformation must be performed again in the control algorithm, to convert the voltage of the d-q axis into a five-phase voltage for the drive bridge.

For the five-phase PMSM, the design, processing, and installation of permanent magnets will make the air-gap magnetic field become non-ideal sinusoidal, with a certain amount of 3rd harmonic components. In addition, some research works artificially inject the 3rd harmonic magnetic potential to improve the power and torque ripple of the motor (Gao et al. (2013); Chen Q. et al. (2022)). Therefore, there will be a non-zero third harmonic current. It is beneficial to consider both the fundamental current and the third harmonic current in the modeling process for the subsequent work.

$$I_{dq} = T I_s = T_{Park} T_{Clarke} I_s \tag{1}$$

where  $T = T_{Park} T_{Clarke}$ ,  $I_{dq} = [i_{d1} \ i_{q1} \ i_{d3} \ i_{q3} \ i_n]^T$ ,  $I_s = [i_a \ i_b \ i_c \ i_d \ i_e]^T$ .

The five-phase motor is a coordinate transformation from the natural coordinate system (*abcde*) to the rotational phase ( $d_1q_1d_3q_3n$ ). This transformation extends the  $abc \rightarrow dqn$  transformation and is used for three-phase to the five-phase case. Usually, the coordinate transformation is divided into two parts: Clarke (*abcde* to  $\alpha_1\beta_1\alpha_3\beta_3z$ ) and Park ( $\alpha_1\beta_1\alpha_3\beta_3z$  to  $d_1q_1d_3q_3n$ ) transformation. Under normal working conditions, the five-phase PMSM extended Clarke transformation matrix is:

$$T_{Clarke} = \begin{bmatrix} 1 & \cos\theta & \cos2\theta & \cos2\theta & \cos\theta \\ 0 & \sin\theta & \sin2\theta & -\sin2\theta & -\sin\theta \\ 1 & \cos2\theta & \cos\theta & \cos\theta & \cos2\theta \\ 0 & -\sin2\theta & \sin\theta & -\sin\theta & \sin2\theta \\ 1 & 1 & 1 & 1 & 1 \end{bmatrix} \tag{2}$$

In the normal working state of the motor, the Park transformation matrix is:

$$T_{Park} = \begin{bmatrix} \cos\theta & \sin\theta & 0 & 0 & 0 \\ -\sin\theta & \cos\theta & 0 & 0 & 0 \\ 0 & 0 & \cos3\theta & \sin3\theta & 0 \\ 0 & 0 & -\sin3\theta & \cos3\theta & 0 \\ 0 & 0 & 0 & 0 & 1 \end{bmatrix} \tag{3}$$

The stator voltage equation of the five-phase PMSM in natural coordinates is (Tian et al. (2018)):

$$U_s = R_s I_s + \frac{d(L_s I_s + \Lambda_m)}{dt} \tag{4}$$

where  $U_s$  and  $I_s$  are the stator voltage and current vectors, respectively.  $R_s$  and  $L_s$  are the stator resistance and stator inductance matrices, respectively.  $\Lambda_m$  is the permanent magnet flux linkage vector represented by its first and third space harmonics, as shown in the following Formula 5.

$$\Lambda_m^{abcde} = \Lambda_1 \begin{bmatrix} \cos\theta \\ \cos(\theta - \delta) \\ \cos(\theta - 2\delta) \\ \cos(\theta + 2\delta) \\ \cos(\theta + \delta) \end{bmatrix} + \Lambda_3 \begin{bmatrix} \cos3\theta \\ \cos3(\theta - \delta) \\ \cos3(\theta - 2\delta) \\ \cos3(\theta + 2\delta) \\ \cos3(\theta + \delta) \end{bmatrix} \tag{5}$$

The electromagnetic torque expression for the five-phase PMSM can be found in (Ge et al. (2018)). Due to the space-time decoupling characteristics of the fundamental wave and 3rd harmonic, the fundamental symmetrical current cannot cause torque ripple. Therefore, the electromagnetic motor torque is given by Equation 6 (Tian et al. (2018)) under the normal state of the motor.

$$T_{em} = \frac{5P_p}{2} (\Lambda_1 i_{q1} + 3\Lambda_3 i_{q3}) \tag{6}$$

where  $P_p$  is the number of pole pairs. The contribution of the third harmonic  $\Lambda_3 i_{q3}$  to the total torque is about 1% (Tian et al. (2018)). In summary, we can control the torque by adjusting  $i_{q1}$ .

## Corrected motor model under fault conditions

If a normal motor model is used in the  $dq$  axis under a single-phase fault, the remaining four-phase currents are unbalanced and distorted. The back EMF will cause fluctuations in speed and torque. The A-phase open-circuit fault can be taken as an example for analysis. Once the A-phase is opened, the five-phase motor is reduced from a five-dimensional symmetrical system to a four-dimensional asymmetrical system. Equation 7 shows the decoupling transformation modified Clarke matrix (Dwari and Parsa (2011)). The derivation of (7) is based on following steps. First, removing the first column element corresponding to A. Second, removing the elements corresponding to the third row of  $i_{d3}$ . Third, modifying the elements to make each row orthogonal to each other.

$$\mathbf{T}'_{\text{Clarke}} = \begin{bmatrix} \cos\theta - 1 & \cos 2\theta - 1 & \cos 2\theta - 1 & \cos\theta - 1 \\ \sin\theta & \sin 2\theta & -\sin 2\theta & -\sin\theta \\ -\sin 2\theta & \sin\theta & -\sin\theta & \sin 2\theta \\ 1 & 1 & 1 & 1 \end{bmatrix} \quad (7)$$

Here, the motor current expression is:

$$\mathbf{I}^{\alpha_1\beta_1\beta_3n} = \mathbf{T}'_{\text{Clarke}} \mathbf{I}^{bcde} \quad (8)$$

For the faulty motor, the third row is deleted in order to correct the Clarke transformation matrix, resulting in the lack of  $i_{\alpha_3}$  component. Therefore, it is not applicable to apply the previous Park transformation only to the  $i_{\beta_3}$  current component. Combining with the modified Clarke transformation, the Park transformation is modified as:

$$\mathbf{T}'_{\text{Park}} = \begin{bmatrix} \cos\theta & \sin\theta & 0 & 0 \\ -\sin\theta & \cos\theta & 0 & 0 \\ 0 & 0 & 1 & 0 \\ 0 & 0 & 0 & 1 \end{bmatrix} \quad (9)$$

The expression form of the stator voltage remains unchanged. Once an open-circuit motor fault occurs in a certain phase of winding, the system dimension decreases. Moreover, the fundamental wave and the third harmonic are no longer decoupled. At this time, the fundamental wave current will interact with the third harmonic magnetic potential to generate torque ripple. The permanent magnet flux linkage can be expressed as:

$$\Lambda_m'^{bcde} = \Lambda_1 \begin{bmatrix} \cos(\theta - \delta) \\ \cos(\theta - 2\delta) \\ \cos(\theta + 2\delta) \\ \cos(\theta + \delta) \end{bmatrix} + \Lambda_3 \begin{bmatrix} \cos 3(\theta - \delta) \\ \cos 3(\theta - 2\delta) \\ \cos 3(\theta + 2\delta) \\ \cos 3(\theta + \delta) \end{bmatrix} \quad (10)$$

The electromagnetic torque equation under fault conditions can also be obtained (Tian et al. (2018)):

$$T_{\text{em}} = \frac{5P_p}{2} \Lambda_1 i_q \left[ 1 + \frac{3\Lambda_3}{2\Lambda_1} (-\cos(2\theta) + \cos(4\theta)) \right] \quad (11)$$

When an open-circuit fault occurs in the winding, the winding structure of the stator is no longer symmetrical. Now, the circular rotating magnetic field can be reconstructed by adjusting the amplitude and phase of the residual phase current. Hence, the motor torque is smooth before and after the fault. The system reliability is also improved.

It can be seen that the basic torque component in Equation 11 is the same as the basic torque component in Equation 6 for normal operation of the motor. According to Equation 11, the existence of the 3rd harmonic magnetic potential after the fault will cause the 2nd and 4th torque ripples. In many cases, due to the small  $\left(\frac{\Lambda_3}{\Lambda_1}\right)$  ratio, these ripples are acceptable. Let the 2nd and 4th torque ripple caused by the 3rd harmonic magnetic potential be 0,  $i_q = C$ , and substitute it into the Formula 1 to obtain the residual phase current. The new reference current enables the system to achieve bumpless operation with minimal torque ripple under fault conditions.

## Optimizing the reference current with the adjustment factor

Simulation results indicate that the system can realize the minimum torque fluctuation and even undisturbed operation under single-phase conditions with open-circuit fault. First, the coordinate transformation matrix is modified. Then, the reset reference current is obtained under the constraint of instantaneous power balance. FTC is theoretically realized, but the amplitude of the fault-tolerant current obtained in this way is seriously unbalanced. Simulation results also show that the residual phase current fluctuates greatly and even doubles the motor's rated current. In practical applications, such a reference current will generate high heat for a long time. It is a big hidden danger to permanent magnets and other working parts. It may cause more secondary severe damage to the motor drive system than an open-circuit fault.

For the above problem of large fluctuation range of residual phase current. Using the idea of vector synthesis, the objective function is to minimize the current fluctuation. The torque fluctuation fluctuates within a small allowable range. The phase current balance is used as the constraint condition. Finally, the adjustment factor  $\alpha$  is optimized. Figure 2 shows the control block diagram of the control system. In Figure 2, the reference current of the motor without faults and the fault-tolerant reference current under the optimal torque is vector synthesized under the  $\alpha$  adjustment factor. Besides, the fault-tolerant reference current is considered. This approach considers the torque ripple under fault and considers the optimal current for motor operation under fault.



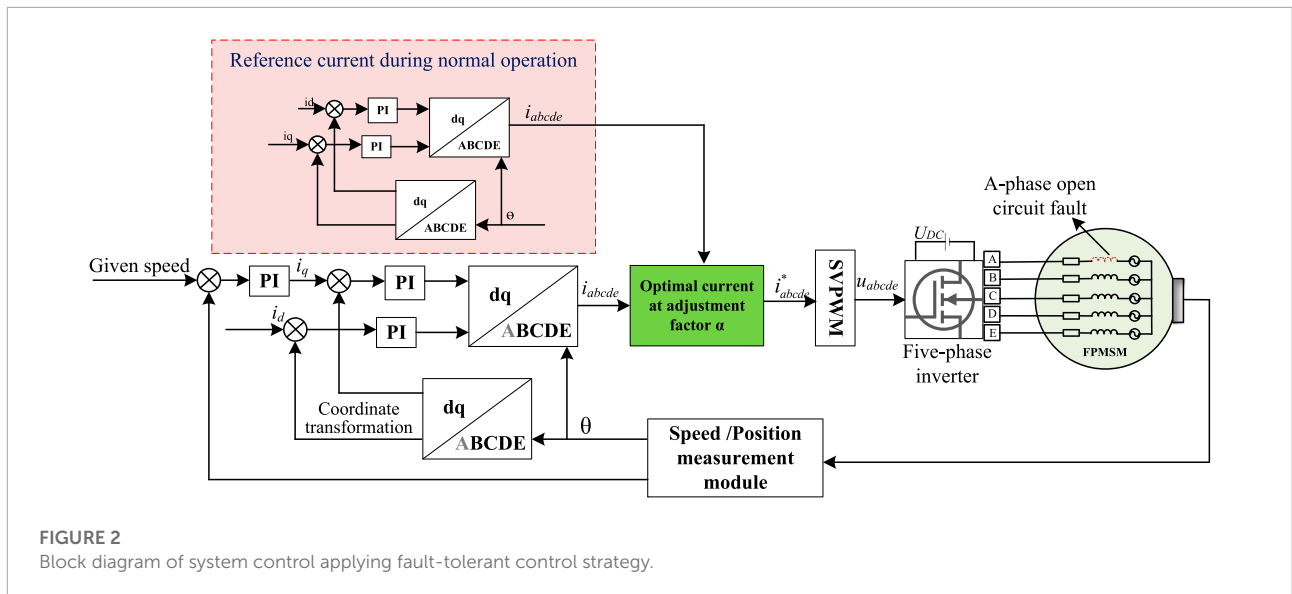


**FIGURE 2**  
Block diagram of system control applying fault-tolerant control strategy.

### Chaotic particle swarm optimization algorithm

The chaotic particle swarm optimization (CPSO) algorithm (Wang et al. (2021)) has the following characteristics. The adaptive inertia weight is used to accelerate the convergence speed, which is improved based on the particle swarm optimization (PSO) algorithm. The system is avoided falling into local optimum by performing chaotic searches in the neighborhood. CPSO can be used to solve parameter optimization problems. The traditional PSO algorithm is prone to premature phenomenon in the solution process. To avoid this shortcoming, CPSO was based on a logistic equation. When the particle falls into the local optimum, a chaotic disturbance is used to jump out of the local optimum.

### Fault-tolerant reference current of fusion chaotic particle swarm optimization algorithm

The above CPSO is applied to optimize the reference current. The optimization idea of CPSO is followed. Once a fault is detected, the system can smoothly switch from the normal working mode to the fault-tolerant running mode without changing the hardware form. The A-phase open-circuit fault is an example. The reference current is optimized by adding adjustment factors in CPSO. The reference current is divided into the current reference  $i_{abcde}$  of the system's normal operation before the fault and the fault-tolerant reference current  $i'_{bcde}$  obtained under the electro-magnetic power balance method. An adjustment factor is set as  $\alpha$ , and optimized reference current  $i^*_{bcde}$

can be expressed as:

$$i^*_{bcde} = \alpha i'_{bcde} + (1 - \alpha) i_{bcde} \tag{12}$$

The chaotic particle swarm is used to adaptively optimize  $\alpha$ , taking the minimum torque fluctuation as the optimization goal, and the optimal torque state corresponds to an optimal  $\alpha$ . The particle swarm variables are:

- 1) Decision variables  $\alpha$ ;
- 2) The minimum torque ripple change is defined as  $\Delta T_{em}$ , then the objective function is:

$$\Delta T_{em} = \min \int_0^T \left| \frac{dT_{em}}{dt} \right| dt \tag{13}$$

The torque fluctuation after fault tolerance is optimized by using the reference current under the fault and the reference current under the normal operation of the motor under the adjustment factor  $\alpha$ .

- 3) Constraints:

$$s.t. \begin{cases} G_j(I^*) = \sum_{j=2}^5 I^* = 0 \\ T_{em} \geq T_L \\ i_{abcde} < i'_{bcde} \end{cases} \tag{14}$$

In (14), the first equation denotes that the obtained reference current must meet and be zero (Chen Z. et al. (2022)). The second inequality is the electromagnetic torque of the motor is greater than the load torque (Li et al. (2014)). The third inequality denotes that the current fluctuation range is smaller than that without fault tolerance after the fault.

The adjustment factor  $\alpha$  is optimized under the above constraints to minimize the torque ripple. This approach

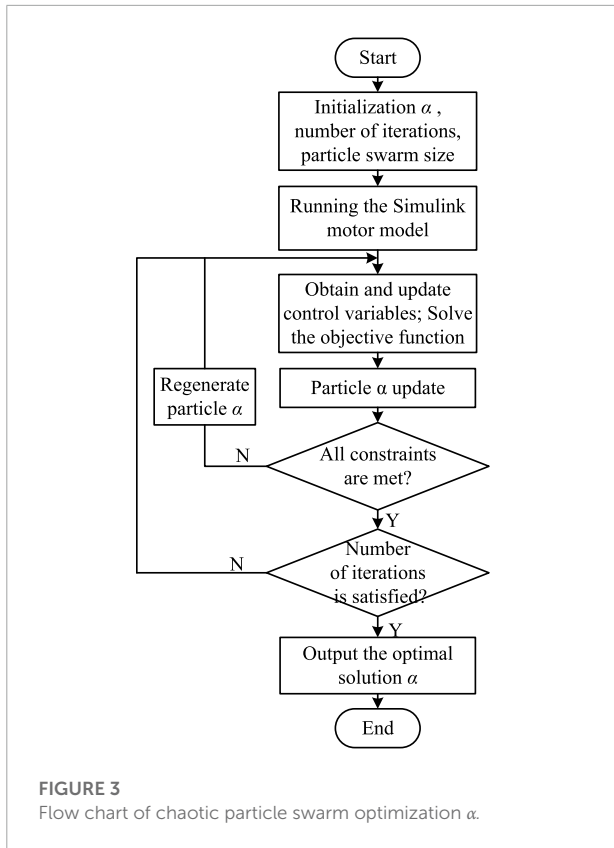


FIGURE 3 Flow chart of chaotic particle swarm optimization  $\alpha$ .

TABLE 1 Parameters of five-phase permanent magnet synchronous motor.

Parameters	Symbol	Value
Pole pairs	$P_p$	4
Fundamental PM flux linkage	$\Psi_{m1}$	0.505 Wb
Third harmonic flux linkage	$\Psi_{m3}$	0.024 Wb
Stator resistance	$R_s$	0.12 $\Omega$
Stator inductance	$L_s$	1.35 mH
Given speed	$n$	1,500 r/min

considers both the torque fluctuation and the current fluctuation range, which is a dual consideration for the safe operation of the motor. Figure 3 presents the flow chart of alpha optimization.

### Simulation and verification

In order to verify the feasibility of the FT-FOC strategy proposed in this paper, it is used for the normal and single phase open-circuit fault conditions of the motor respectively. Comparisons are carried out with the fault-tolerant reference current based on different adjustment factors  $\alpha$ . The five-phase PMSM parameters are shown in Table 1.

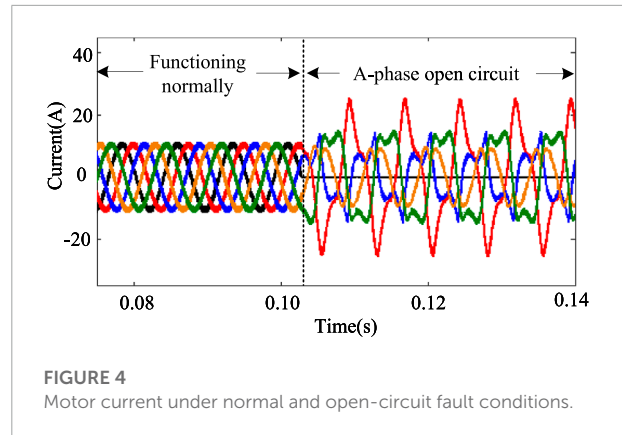


FIGURE 4 Motor current under normal and open-circuit fault conditions.

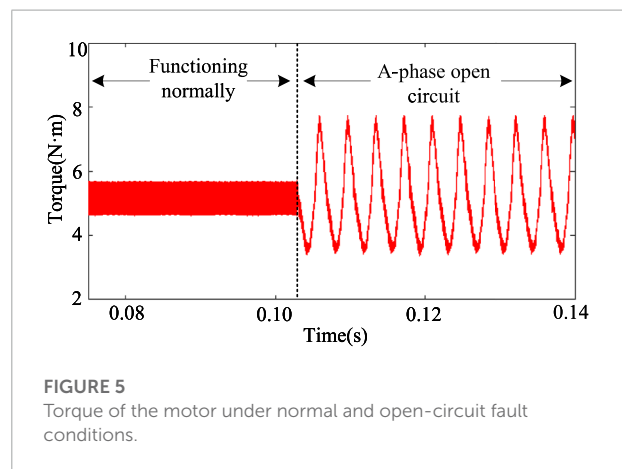


FIGURE 5 Torque of the motor under normal and open-circuit fault conditions.

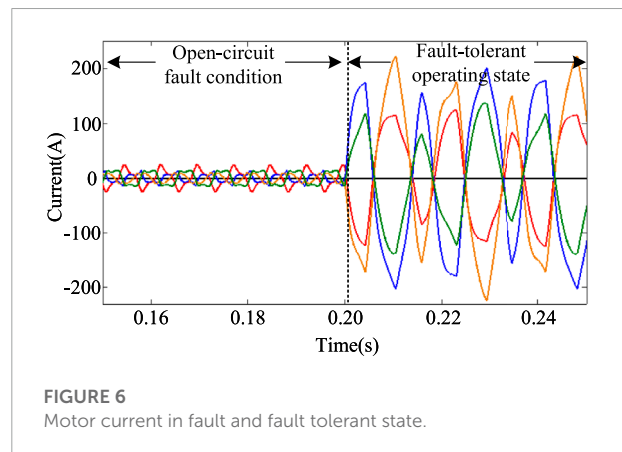
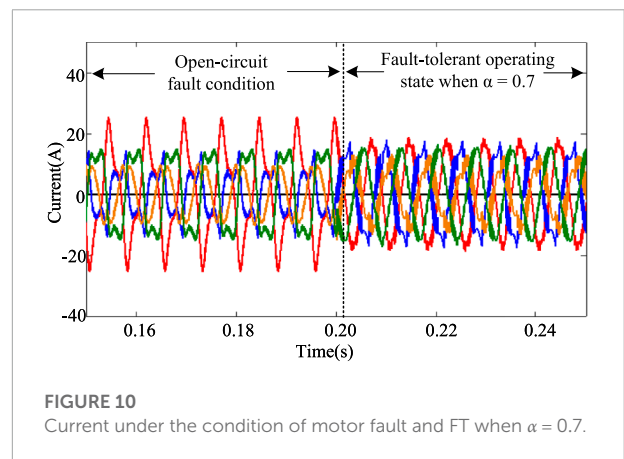
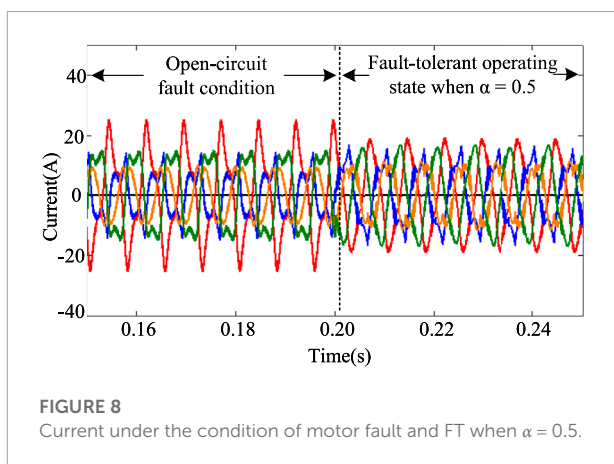
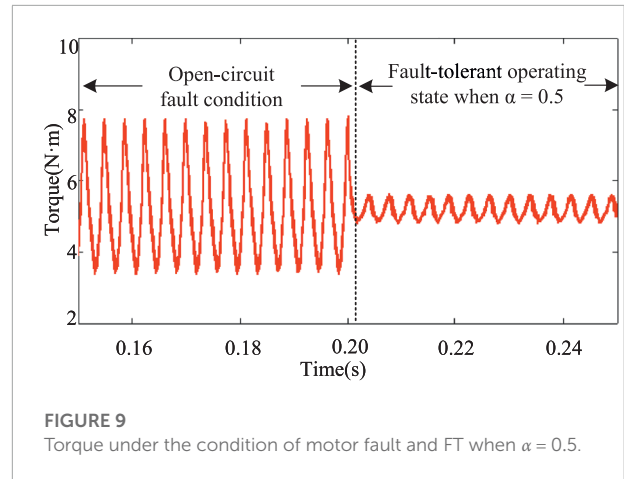
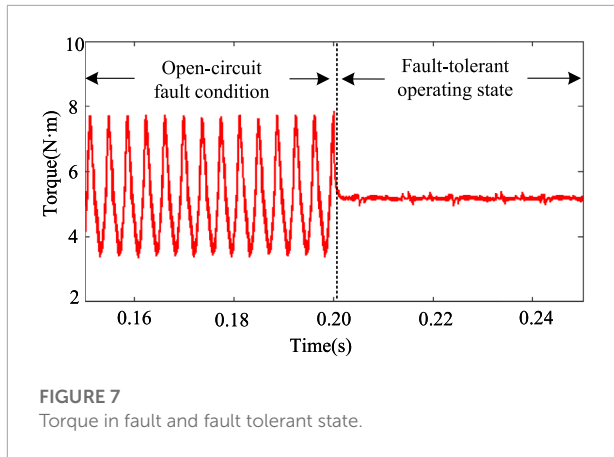


FIGURE 6 Motor current in fault and fault tolerant state.

The current, electromagnetic torque and rotational speed curves of the motor under normal and A-phase open-circuit fault states are shown in Figure 4 and Figure 5 respectively.

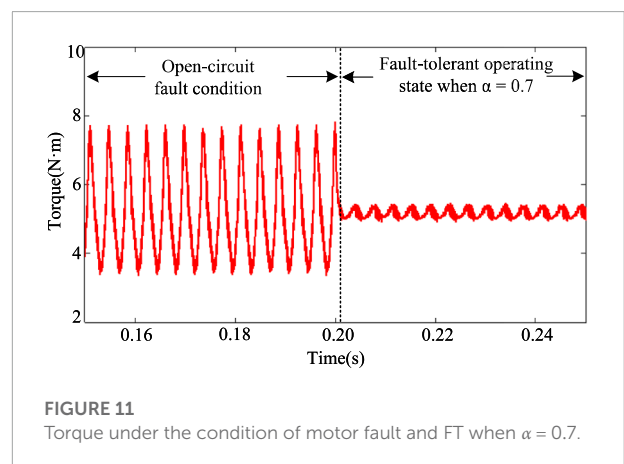
When the coordinate transformation is used, the current electromagnetic torque waveforms of the motor in the fault and fault-tolerant operation state are shown in Figure 6 and Figure 7, where  $\alpha = 0$ .



In the normal operation state of the motor, the torque fluctuation range of the motor is  $1\text{N}\cdot\text{m}$ . After the open-circuit fault of phase A occurs, the torque fluctuation range is  $4\text{N}\cdot\text{m}$ , which is 4 times that of normal operation. When the fault-tolerant current is used as the reference current, the torque fluctuation range is  $0.5\text{N}\cdot\text{m}$ , where the optimization effect is remarkable. However, because of the imbalance of the effective value of each phase current, the current fluctuates greatly. The chaotic particle swarm optimization algorithm is used to optimize the current adaptively under the adjustment factor  $\alpha$  equal to 0.5 and 0.7, respectively. The simulation results of the current and electromagnetic torque of the motor operation are shown in **Figures 8–11**.

In order to further illustrate the current fluctuation of the motor under different adjustment factors, the relationship is obtained between the adjustment factor and the current range from the simulation experiment. The relationship is shown in **Table 2**.

It can be seen from the table that in different applications, the safe operation range of the open-circuit fault and the



corresponding torque fluctuation can be selected to meet the safe operation of the motor. Meanwhile, the motor runs reliably and smoothly under acceptable conditions for fluctuations after a fault occurs.

TABLE 2 Relationship between different adjustment factors and current range and torque ripple.

$\alpha$	Current range(A)	Torque range (N·m)
0.1	$\pm 23$	4.0~6.5
0.2	$\pm 20$	4.4~6.1
0.3	$\pm 20$	4.5~5.9
0.4	$\pm 18$	4.9~5.5
0.5	$\pm 18$	4.8~5.4
0.6	$\pm 18$	4.8~5.5
0.7	$\pm 18$	4.8~5.4
0.8	$\pm 19$	4.9~5.4
0.9	$\pm 25$	4.9~5.4
0	$\pm 223$	4.5~5.5
1.0	$\pm 25$	3.5~7.5

## Conclusion

Compared with the previous related research, the main contributions of this paper are as follows. First, the fault-tolerant current is adaptively optimized by the chaotic particle swarm optimization algorithm. The current fluctuation is also considered on the premise of considering the torque fluctuation. The adaptive optimization of the current by the CPSO achieves the effect of filtering and reducing the amplitude of the fault-tolerant current after a fault. From the current point of view, the dimension of the safe operation of the motor is increased. Second, the proposed FT-FOC control strategy has the advantage of maintaining the exact same control structure before and after failure. This ensures a very smooth transition of the system to fault-tolerant mode. Finally, simulation verified that the proposed FTC strategy could reduce the torque pulsation when a fault occurs and ensure that the dynamic performance reaches the normal state level. It can also ensure that the fault-tolerant current range is basically the same as the current range before the fault, which enhances the robustness of the system against external interference.

To sum up, the field-oriented FTC strategy adopted in this paper considers the two motor operating parameters of torque and current simultaneously, which broadens the dimension of reliable operation of the system.

## References

- Chen, F., Hua, W., Huang, W., Zhu, J., and Tong, M. (2019). Open-circuit fault-tolerant strategies for a five-phase flux-switching permanent magnet motor based on model predictive torque control method. *Proc. CSEE* 39, 337–346. doi:10.13334/j.0258-8013.pcsee.181802
- Chen, Q., Xia, Y., Zhao, W., and Liu, G. (2022a). Open-circuit fault-tolerant control for five-phase permanent magnet motors with trapezoidal back-emf by deadbeat current tracking. *Trans. China Electrotech. Soc.* 37, 368–379. doi:10.19595/j.cnki.1000-6753.tces.200897
- Chen, Y., Yang, Z., Zhou, H., Ji, C., and Li, P. (2021). Pmsm open circuit fault tolerance control. *Electr. Mach. Control* 25, 11–16. doi:10.15938/j.emc.2021.09.002
- Chen, Z., Zhang, X., Liu, C., Zhang, H., and Luo, G. (2022b). Research on current decoupling and harmonic suppression strategy of permanent magnet synchronous motor by proportional resonance adaptive disturbance rejection control. *Proc. CSEE* 1. doi:10.13334/j.0258-8013.pcsee.211791

## Data availability statement

The original contributions presented in the study are included in the article/Supplementary Material, further inquiries can be directed to the corresponding author.

## Author contributions

CC, YS, and YZ contributed to conception and design of the study. JT and SG organized the database. CC and YS performed the simulation and statistical analysis. CC wrote the first draft of the manuscript. YS and BL wrote sections of the manuscript. All authors contributed to manuscript revision, read, and approved the submitted version.

## Funding

This work was supported by the Shaanxi Province Key Research and Development Program under Grant (No. 2021GY-149), Shaanxi Province Science and Technology Innovation Guidance Special (Fund) Project under Grant (No. 2022QFY01-16), the National Natural Science Foundation of China (No. 61833013), and the Natural Sciences and Engineering Research Council of Canada.

## Conflict of interest

The authors declare that the research was conducted in the absence of any commercial or financial relationships that could be construed as a potential conflict of interest.

## Publisher's note

All claims expressed in this article are solely those of the authors and do not necessarily represent those of their affiliated organizations, or those of the publisher, the editors and the reviewers. Any product that may be evaluated in this article, or claim that may be made by its manufacturer, is not guaranteed or endorsed by the publisher.

- Dwari, S., and Parsa, L. (2011). Fault-tolerant control of five-phase permanent-magnet motors with trapezoidal back emf. *IEEE Trans. Ind. Electron.* 58, 476–485. doi:10.1109/TIE.2010.2045322
- Fnaiech, M. A., Betin, F., Capolino, G.-A., and Fnaiech, F. (2010). Fuzzy logic and sliding-mode controls applied to six-phase induction machine with open phases. *IEEE Trans. Ind. Electron.* 57, 354–364. doi:10.1109/TIE.2009.2034285
- Gaeta, A., Scelba, G., and Consoli, A. (2013). Modeling and control of three-phase pmsms under open-phase fault. *IEEE Trans. Ind. Appl.* 49, 74–83. doi:10.1109/TIA.2012.2228614
- Gao, H., Yang, G., Liu, J., and Zhao, P. (2013). Air-gap mmf analysis for five-phase pmsm with third harmonic injection. *Electr. Mach. Control* 17, 1–6. doi:10.15938/j.emc.2013.10.005
- Ge, Q., Tian, B., Sun, L., An, Q., and Zhao, K. (2018). Unified foc of five-phase permanent magnet motor under open-circuit conditions. *Electr. Power Autom. Equip.* 38, 192–200. doi:10.16081/j.issn.1006-6047.2018.02.025
- Huang, W., Du, J., Hua, W., and Fan, Q. (2021). An open-circuit fault diagnosis method for pmsm drives using symmetrical and dc components. *Chin. J. Electr. Eng.* 7, 124–135. doi:10.23919/CJEE.2021.000031
- Li, Y., Lu, H., Qu, W., and Sheng, S. (2014). A permanent magnet synchronous motor current suppression method based on resonant controllers. *Proc. CSEE* 34, 423–430. doi:10.13334/j.0258-8013.pcsee.2014.03.013
- Liu, X., Wang, Z., Wang, W., Lv, Y., Yuan, B., Wang, S., et al. (2022). Smo-based sensorless control of a permanent magnet synchronous motor. *Front. Energy Res.* 10, 1–10. doi:10.3389/fenrg.2022.839329
- Liu, X., Zeng, Z., and Wunsch Ii, D. C. (2020). Memristor-based LSTM network with *in situ* training and its applications. *Neural Netw.* 40, 300–311. doi:10.1016/j.neunet.2020.07.035
- Okedu Kenneth, E., and Barghash, H. (2021). Enhancing the transient state performance of permanent magnet synchronous generator based variable speed wind turbines using power converters excitation parameters. *Front. Energy Res.* 9, 1–10. doi:10.3389/fenrg.2021.655051
- Salehifar, M., Arashloo, R., Moreno-Equilaz, J., Sala, V., and Romeral, L. (2014). Fault detection and fault tolerant operation of a five phase pm motor drive using adaptive model identification approach. *IEEE J. Emerg. Sel. Top. Power Electron.* 2, 212–223. doi:10.1109/JESTPE.2013.2293518
- Tao, T., Zhao, W., Cheng, M., and Wang, Z. (2019). Overview of fault tolerant control and its key technologies for polyphase motors. *CJEE* 39, 316–326. doi:10.13334/j.0258-8013.pcsee.181589
- Tian, B., Mirzaeva, G., An, Q., Sun, L., and Semenov, D. (2018). Fault-tolerant control of a five-phase permanent magnet synchronous motor for industry applications. *IEEE Trans. Ind. Appl.* 54, 3943–3952. doi:10.1109/tia.2018.2820060
- Wang, X., Fu, X., Dong, J., and Jiang, J. (2021). Dynamic modified chaotic particle swarm optimization for radar signal sorting. *IEEE Access* 9, 88452–88466. doi:10.1109/ACCESS.2021.3091005
- Wu, X., Song, W., and Xue, C. (2019). Direct torque control schemes for five-phase permanent magnet synchronous machines based on duty ratio optimization of virtual voltage vector sets. *Proc. CSEE* 39, 857–867. doi:10.13334/j.0258-8013.pcsee.170953
- Zhang, C., Zhao, S., and He, Y. (2021). An integrated method of the future capacity and rul prediction for lithium-ion battery pack. *IEEE Trans. Veh. Technol.* 71, 2601–2613. doi:10.1109/TVT.2021.3138959
- Zhao, S., Zhang, C., and Wang, Y. (2022). Lithium-ion battery capacity and remaining useful life prediction using board learning system and long short-term memory neural network. *J. Energy Storage* 52, 104901. doi:10.1016/j.est.2022.104901
- Zhao, W., Cheng, M., Hua, W., Jia, H., and Cao, R. (2011). Back-emf harmonic analysis and fault-tolerant control of flux-switching permanent-magnet machine with redundancy. *IEEE Trans. Ind. Electron.* 58, 1926–1935. doi:10.1109/TIE.2010.2050758
- Zhou, X., Sun, J., Li, H., and Song, X. (2019). High performance three-phase pmsm open-phase fault-tolerant method based on reference frame transformation. *IEEE Trans. Ind. Electron.* 66, 7571–7580. doi:10.1109/TIE.2018.2877197